Cellulose (2014) 21:3323–3338
DOI 10.1007/s10570-014-0383-3

ORIGINAL PAPER

Synthesis and crystallization-induced microphase separation of cellulose triacetate-*block*-poly(γ-benzyl-L-glutamate)

Hiroshi Kamitakahara · Akihiro Baba · Arata Yoshinaga · Ryo Suhara · Toshiyuki Takano

Received: 18 February 2014 / Accepted: 28 July 2014 / Published online: 3 August 2014

Abstract This article describes the first observation of crystallization-induced microphase separation in thin film and bulk cellulose triacetate-*block*-poly (γ-benzyl-L-glutamate) (PBLG) [cellulose triacetate (CTA)-*b*-PBLG] via copper-catalyzed azide–alkyne cycloaddition (CuAAC) between azido-functionalized CTA at the reducing end and alkyne-functionalized PBLG at the C-terminus. The reactivity of the amino group at the C-1 position of the glucosyl residue at the reducing end for the initiation reaction of the ring-opening polymerization (ROP) of γ-benzyl-L-glutamate *N*-carboxyanhydride was compared to that of the azido group at the reducing end of CTA for CuAAC, with PBLG bearing an alkyne group at the C-terminus. Although the amino group at the reducing end of CTA exhibited no reactivity as a macroinitiator for ROP of BLG, the azido group at the reducing end of CTA reacted with the alkyne group at the C-terminus of PBLG to afford CTA-*b*-PBLG. The structure of CTA-*b*-PBLG was characterized by ^{1}H- and ^{13}C-nuclear magnetic resonance spectroscopies, infrared spectroscopy, differential scanning calorimetry, and wide angle X-ray diffractometry. Microphase separation of the film and bulk of CTA-*b*-PBLG was clearly shown by atomic force microscopy, field-emission scanning electron microscopy, and transmission electron microscopy.

Keywords Diblock copolymer · Cellulose triacetate (CTA) · Poly(benzyl-L-glutamate) (PBLG) · Copper-catalyzed azide–alkyne cycloaddition · Microphase separation

Introduction

This study aims to prepare the first cellulosic diblock copolymer exhibiting microphase separation in the bulk. Microphase separation in cellulosic materials remains unexplored, although the microphase separation of block copolymers has received considerable attention because its bottom-up process to build nano patterns allows us to produce new materials with fascinating features.

Since the 1960s, some researchers have studied cellulosic diblock copolymers of cellulose esters (Kim et al. 1973, 1976; Pohjola and Eklund 1977; Mezger and Cantow 1983a, b, 1984; Lonikar et al. 1990; de Oliveira and Glasser 1994; Kadokawa et al. 1996; Kamatani and Kikuchi 2002; Jadage et al. 2004; Kamitakahara and Nakatsubo 2005; Kamitakahara et al. 2005), cellulose ethers (Ceresa 1961; Feger and Cantow 1980; Jadage et al. 2004), and unsubstituted

Electronic supplementary material The online version of this article (doi:10.1007/s10570-014-0383-3) contains supplementary material, which is available to authorized users.

H. Kamitakahara (✉) · A. Baba · A. Yoshinaga · R. Suhara · T. Takano
Graduate School of Agriculture, Kyoto University, Sakyo-ku, Kyoto 606-8502, Japan
e-mail: hkamitan@kais.kyoto-u.ac.jp

cellulose (Enomoto et al. 2006; Yagi et al. 2010; Sakaguchi et al. 2010; Enomoto-Rogers et al. 2011). Our group has focused on the synthesis of cellulose triacetate (CTA)-based diblock copolymers with well-defined structures, such as CTA-*b*-Nylon 15, via a stepwise reaction of an ω-azido-functionalized acyl halide with tri-*O*-acetyl-cellulosylamine. Cellulose acetate membranes (Edgar et al. 2001; Hiratsuka et al. 1994; Kubota et al. 2003; Machii et al. 2004, 2005) are of great importance for medical treatments such as artificial dialysis. Microphase-separated cellulose acetate membrane will therefore be a prime candidate for the separation of biologically valuable molecules from blood in the future.

Here, we describe the synthesis of cellulose triacetate-*block*-poly(γ-benzyl-L-glutamate) (CTA-*b*-PBLG). Lonikar et al. reported the anionic polymerization of γ-benzyl-L-glutamate *N*-carboxyanhydride (NCA)-initiated amino-terminated CTA oligomers to afford cellulosic block copolymer of CTA and PBLG (Lonikar et al. 1990). They treated cellulose triacetate with conc. H_2SO_4 and a small amount of H_2O to afford hydroxy-terminated CTA oligomers. The hydroxy-terminated CTA oligomers must have two hydroxyl groups at both ends of cellulose triacetate. *m*-Nitrophenyl isocyanate was reacted with those two hydroxyl groups to afford nitro-terminated CTA oligomers. The amino-terminated CTA oligomers were obtained by hydrogenating the nitro-terminated CTA oligomers. Lonikar et al. hydrolyzed ester groups to afford a block copolymer of cellulose and poly(L-glutamic acid) but did not report any characteristics of the block copolymer of CTA and PBLG (Lonikar et al. 1990).

Poly(γ-benzyl-L-glutamate) (PBLG) has an α-helical structure, resulting in a rigid rod architecture of its homo- and co-polymers, and its blends display gas permeability (Vivatpanachart et al. 1981; Kang et al. 1988), liquid crystallinity (Toriumi et al. 1979, 1980, 1981, 1983; Toriumi and Uematsu 1984; Uematsu and Uematsu 1984; Sanefuji et al. 1985; Ando et al. 1987), and optical (Toriumi and Uematsu 1984; Tsai et al. 1990; Weiss et al. 1992; Floudas et al. 2003; Ibarboure et al. 2007) and piezoelectric (Farrar et al. 2010) properties, making them promising as high performance materials. The CTA and PBLG segments exhibit crystallizable and α-helical structures, respectively. Thus, crystallization-driven microphase separation of a diblock copolymer (Chen 2013) is applicable to CTA-*b*-PBLG.

Our strategy to accomplish the synthesis of CTA-*b*-PBLG includes two individual methodologies: a dimeric cellobiose acetate is used to model the polymeric cellulose triacetate (CTA) block; a study is performed on the reactivities of functional end groups such as amino and azido groups of di- and polysaccharide blocks to synthesize CTA-*b*-PBLG by a ring-opening polymerization of γ-benzyl-L-glutamate *N*-carboxyanhydride (BLG NCA) and by a coupling reaction with alkyne-functionalized PBLG segment via copper-catalyzed azide–alkyne cycloaddition (CuAAC). We describe four combinations, including two different carbohydrate blocks and two methods, to prepare diblock copolymers.

The thin film and bulk morphologies of CTA-*b*-PBLG on the nanometer scale were observed by means of field-emission scanning electron microscopy (FE-SEM) and transmission electron microscopy (TEM). After annealing at a temperature higher than the cold crystallization temperature of the CTA segment, CTA-*b*-PBLG was stained by RuO_4 vapor, which selectively stains double bonds in benzyl groups.

This article discusses the synthesis method of CTA-*b*-PBLG and the morphological observation of the nanostructures of phase-separated CTA-*b*-PBLG, induced by the crystallization of the CTA segment.

Materials and methods

Materials

All reagents and solvents were obtained from Nacalai tesque, Wako Chemical, and Sasaki Chemical, Japan, and were used as received.

Measurements

^1H and ^{13}C NMR spectra were acquired in $CDCl_3$ or in $CDCl_3$ with 15 % trifluoroacetic acid on a Varian 500 NMR spectrometer at room temperature. The molecular weights of the products were measured by gel permeation chromatography (GPC) in chloroform on a Shimadzu SEC system (CBM-20A, SPD-10A_{VP}, SIL-10A, LC-10AT_{VP}, FCV-10AL_{VP}, CTO-10A_{VP}, RID-10A, and FRC-10A, Shimadzu, Japan). The sample solutions were passed through a syringe filter (Sartorius Stedim, Minisart RC 4 or RC 15; pore size 0.45 μm, or Whatman Grade GF/D; pore size 2.7 μm)

before GPC analysis. Shodex columns (K802, K802.5, and K805) with a guard column (Shodex, K-G) were used. Number and weight averaged molecular weights (M_n and M_w) and polydispersity indices (M_w/M_n) were estimated using polystyrene standards (Shodex). Matrix-assisted laser desorption/ionization time-of-flight mass (MALDI-TOF MS) spectra were recorded on a Bruker Autoflex III in the positive ion, and linear or reflector modes. 2,5-Dihydroxybenzoic acid (DHB) was used as a matrix for the measurements. Infrared spectra were recorded on a Shimadzu IR Prestage-21 FT spectrophotometer with KBr pellets (4,000–500 cm^{-1}). Differential scanning calorimetry (DSC) thermograms were recorded on DSC823^e (Mettler Toledo, Zurich, Switzerland) with a MultiSTAR HSS7 DSC sensor under a nitrogen atmosphere. A sample in a crucible was heated from −40 to 210 °C at 5 °C/min and cooled to −40 °C at 50 °C/min three times and then heated from −40 to 290 °C at 5 °C/min and cooled to −40 °C at 50 °C/min three times. Appropriate heating runs were recorded for each sample. Wide-angle X-ray scattering measurements were carried out on a Rigaku Ultima IV diffractometer. Nickel-filtered Cu Kα radiation was used at 40 kV and 40 mA.

Synthesis of 2,3,4,6-tetra-*O*-acetyl-β-D-glucopyranosyl-(1 → 4)-2,3,6-tri-*O*-acetyl-β-D-glucopyranosylamine (1, C2TA-NH_2)

The synthesis of C2TA-NH_2 (**1**) was performed as previously described (Kamitakahara and Nakatsubo 2005).

Synthesis of tri-*O*-acetyl cellulosylamine (2, CTA-NH_2)

Tri-*O*-acetyl cellulosylazide (**4**) was hydrogenated by 10 % Pd/C under a hydrogen atmosphere to afford tri-*O*-acetyl cellulosylamine (**2**) according to our previous report (Kamitakahara et al. 2005). Total yield from cellulose: 67 %; number-averaged molecular weight: 1.04×10^4; weight-averaged molecular weight: 1.84×10^4; $DP_n = 35.9$.

Synthesis of 2,3,4,6-tetra-*O*-acetyl-β-D-glucopyranosyl-(1 → 4)-2,3,6-tri-*O*-acetyl-β-D-glucopyranosylazide (3, C2TA-N_3)

The synthesis of C2TA-N_3 (**3**) was carried out as previously described (Kamitakahara and Nakatsubo 2005).

Synthesis of tri-*O*-acetyl cellulosylazide (4, CTA-N_3)

Tri-*O*-acetyl cellulosylazide (**4**) was prepared from cellulose (Avicel, CF-11) according to our previous report (Kamitakahara et al. 2005). Total yield from cellulose: 65 %; number-averaged molecular weight: 1.21×10^4; weight-averaged molecular weight: 2.41×10^4; $DP_n = 41.6$; DSC: $T_g = 144$ °C (heating rate: 5 °C/min); $T_m = 296$ °C (heating rate: 10 °C/min).

Synthesis of γ-benzyl-L-glutamate *N*-carboxyanhydride (5, BLG NCA)

γ-Benzyl-L-glutamate *N*-carboxyanhydride (**5**) was prepared according to the literature (Daly and Poche 1988). To a solution of γ-benzyl-L-glutamate (BLG, 999.9 mg) in anhydrous tetrahydrofuran (15 mL), triphosgene (620.0 mg) was added, and the reaction mixture was stirred at 50 °C for 1.5 h. Tetrahydrofuran was slightly evaporated to afford a concentrated solution of the reaction mixture: note that it should not be concentrated to dryness. *n*-Hexane (50 mL) was added to the solution, and the mixture was kept at −30 °C overnight. The produced crude crystals were filtered and washed with cold *n*-hexane. The crude crystals were recrystallized from ethyl acetate/*n*-hexane (1/1, v/v), filtered off, and washed with cold *n*-hexane to afford BLG NCA (**5**) as colorless crystals (1,048.1 mg, 95 % yield). 500 MHz ^{1}H-NMR ($CDCl_3$): δ 2.20 (m, 2H, CβH_2), 2.60 (t, 2H, $J = 7.0$, CγH_2), 4.38 (t, 1H, $J = 6.0$, CαH), 5.14 (s, 2H, OCH_2Ph), 6.56 (s, 1H, NH), 7.33–7.40 (m, 5H, $OCH_2C_6H_5$), 125 MHz ^{13}C-NMR ($CDCl_3$): δ 26.9 (Cβ), 29.9 (Cγ), 56.9 (Cα), 67.1 (OCH_2Ph), 128.4, 128.6, 128.7, 135.2 (aromatic C), 151.7 (NHC=O), 169.3 (Cδ=O), 172.4 (CαC=O).

Synthesis of 2,3,4,6-tetra-*O*-acetyl-β-D-glucopyranosyl-(1 → 4)-2,3,6-tri-*O*-acetyl-β-D-glucopyranosylamine-*block*-poly(γ-benzyl-L-glutamate) (6) by ring-opening polymerization (ROP) of BLG NCA (5)

C2TA-NH_2 (**1**) (3.3 mg) and BLG NCA (**5**) (20.2 mg) were overnight dried in a glass tube with a side arm on a vacuum line. *N*,*N*-dimethylformamide (DMF, 0.4 mL) was dried over calcium hydride and degassed

by a freeze–pump–thaw cycle, stirred at r.t. overnight, and degassed again by five freeze–pump–thaw cycles. The degassed DMF was loaded into the glass tube where BLG NCA (**5**) was placed, and the solution was further degassed by three freeze–pump–thaw cycles. C2TA-NH_2 (**1**) in a side arm was added to the solution of BLG NCA (**5**) in DMF. The reaction mixture was stirred at r.t. for 24 h and then poured into a large excess of methanol. The resulting precipitate was collected by centrifugation (15,000 rpm, 10 min) to afford crude 2,3,4,6-tetra-*O*-acetyl-β-D-glucopyranosyl-(1 → 4)-2,3,6-tri-*O*-acetyl-β-D-glucopyranosylamine-*block*-poly(γ-benzyl-L-glutamate) (**6**) (20.2 mg). A part of crude compound **6** (13.9 mg) was purified by gel filtration column chromatography LH-20 (eluent: methanol/dichloromethane = 1/4, v/v) to give compound **6** (11.3 mg, 70 % yield (81 % yield from crude compound **6**)). MALDI-TOF MS analysis revealed the existence of PBLGs with amino and pyroglutamate (Habraken et al. 2011) end-groups. MALDI-TOF MS (positive reflector mode, DHB used as a matrix): amino end-group series, *m/z* DP = 2, $[M + Na]^+$ = 1,095.203, $[M + K]^+$ = 1,111.184; DP = 3, $[M + Na]^+$ = 1,314.226, $[M + K]^+$ = 1,330.193; DP = 4, $[M + Na]^+$ = 1,533.308, $[M + K]^+$ = 1,549.290; DP = 5, $[M + Na]^+$ = 1,752.489, $[M + K]^+$ = 1,768.478; DP = 6, $[M + Na]^+$ = 1,971.757, $[M + K]^+$ = 1,987.751; DP = 7, $[M + Na]^+$ = 2,191.115, $[M + K]^+$ = 2,207.112; DP = 8, $[M + Na]^+$ = 2,410.532, $[M + K]^+$ = 2,426.537; DP = 9, $[M + Na]^+$ = 2,590.944, $[M + K]^+$ = 2,606.934; DP = 10, $[M + K]^+$ = 2,826.570, pyroglutamate end-group series, *m/z* DP = 2, $[M + Na]^+$ = 987.233, $[M + K]^+$ = 1,003.195; DP = 3, $[M + Na]^+$ = 1,206.199, $[M + K]^+$ = 1,222.174; DP = 4, $[M + Na]^+$ = 1,425.238, $[M + K]^+$ = 1,441.221; DP = 5, $[M + Na]^+$ = 1,644.371, $[M + K]^+$ = 1,660.361; DP = 6, $[M + Na]^+$ = 1,863.601, $[M + K]^+$ = 1,879.590; DP = 7, $[M + Na]^+$ = 2,082.913, $[M + K]^+$ = 2,098.907; DP = 8, $[M + Na]^+$ = 2,302.307, $[M + K]^+$ = 2,319.284; DP = 9, $[M + Na]^+$ = 2,521.808, $[M + K]^+$ = 2,537.851; DP = 10, $[M + Na]^+$ = 2,742.317, $[M + K]^+$ = 2,757.457; DP = 11, $[M + Na]^+$ = 2,961.135, $[M + K]^+$ = 2,977.204. The molecular weight in $CHCl_3$ was estimated by GPC. Number-averaged molecular weight: 2.7×10^3; weight-averaged molecular weight: 5.2×10^3; DP_n calculated by ^{1}H-NMR measured in $CDCl_3$: 59.4. 500 MHz ^{1}H-NMR ($CDCl_3$): δ 2.0–2.2 (CH_3CO), 2.28 (Hβ), 2.60 (Hγ), 3.93 (Hα), 5.04 (OCH_2Ph), 7.2–7-4 (aromatic H), 8.35 (NH). 125 MHz ^{13}C-NMR ($CDCl_3$): δ 20.5 (CH_3CO), 25.6 (Cβ), 30.9 (Cγ), 56.9 (Cα), 66.2 (OCH_2Ph), 128.1, 128.4, 128.5, 128.5, 128.6, 136.0 (aromatic C), 172.1 (Cδ=O), 175.4 (CαC=O). Note that the carbon resonances of the cellobiosyl residue were hidden in the baseline noise.

Synthesis of alkyne-functionalized poly(γ-benzyl-L-glutamate) (**7**)

Alkyne-functionalized poly(γ-benzyl-L-glutamate) (**7**) was prepared according to the literature (Agut et al. 2008). BLG NCA (**5**, 1,048.1 mg, 3.98 mmol, 13.4 equiv.) was dried in a two-necked flask on a vacuum line. Pre-activated molecular sieves 4 Å (5 g) were added to *N*,*N*-dimethylformamide (DMF, 30 mL) in a second two-necked flask. DMF was degassed by a freeze–pump–thaw cycle, stirred at r.t. overnight, and degassed again by five freeze–pump–thaw cycles. The degassed DMF was loaded into the two-necked flask where BLG NCA (**5**) was placed, and the solution was further degassed by three freeze–pump–thaw cycles. Propargylamine (3-amino-1-propyne, 19 μL, 2.97×10^{-1} mmol, 1 equiv.) was added to the solution of BLG NCA in DMF, and the reaction mixture was stirred at r.t. for 3 days. The reaction mixture was added into a large excess of methanol, and the precipitate was collected by centrifugation (15,000 rpm, 10 min) to afford alkyne-functionalized poly(γ-benzyl-L-glutamate) (**7-2**) (624.0 mg, 60.0 % yield) to be used in a reaction with compound **4**. Number-averaged degree of polymerization (DP_n) calculated by ^{1}H-NMR measured in $CDCl_3$ with 15 % trifluoroacetic acid: 47.1; molecular weight estimated by GPC: number-averaged molecular weight: 2.2×10^3; weight-averaged molecular weight: 3.4×10^3. Proton and carbon resonances excluding those of the end groups were assigned according to the literature (Wang et al. 2008; Caillol et al. 2003). MALDI-TOF MS (positive reflector mode, DHB used as a matrix): pyroglutamate end-group series, *m/z* DP = 8, $[M + Na]^+$ = 1,943.929; DP = 9, $[M + Na]^+$ = 2,163.779; DP = 10, $[M + Na]^+$ = 2,283.119; DP = 11, $[M + Na]^+$ = 2,602.175; DP = 12, $[M + Na]^+$ = 2,821.954; DP = 13, $[M + Na]^+$ = 3,041.011; DP = 14, $[M + Na]^+$ = 3,260.079; DP = 15, $[M + Na]^+$ = 3,479.144; DP = 16, $[M + Na]^+$ = 3,698.961; DP = 17, $[M + Na]^+$ = 3,917.861; DP = 18, $[M + Na]^+$ = 4,136.989;

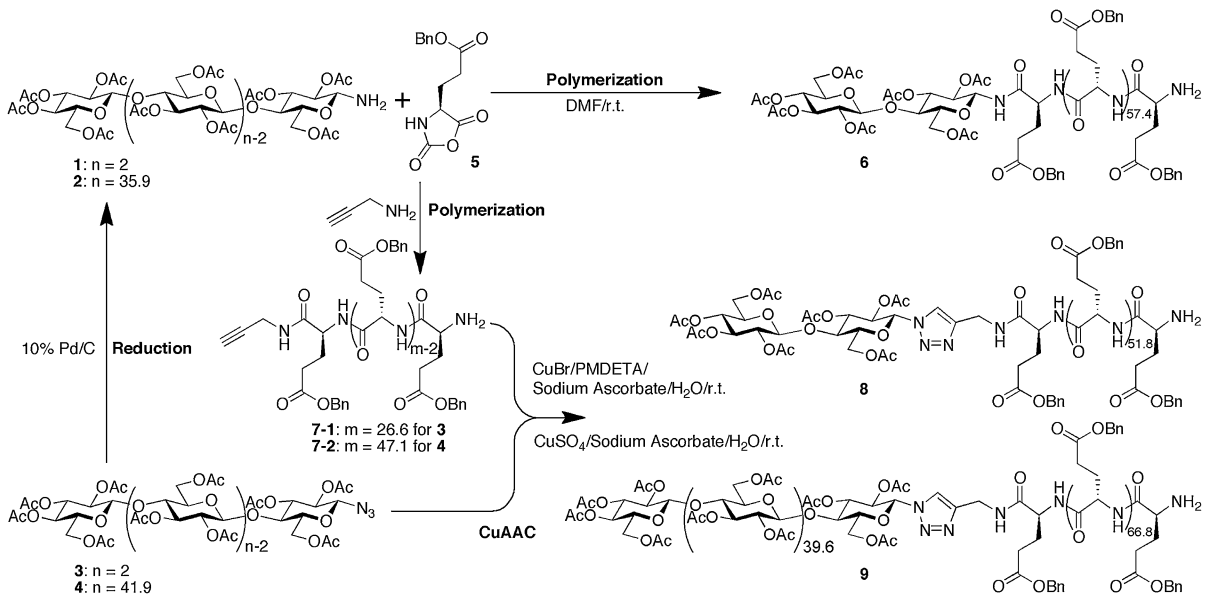

Scheme 1 Synthesis routes for C2TA-*b*-PBLG (**6**) via ring-opening polymerization of BLG NCA (**5**) initiated from amino-functionalized cellulose derivatives (**1**) and for C2TA-*b*-PBLG (**8**) and CTA-*b*-PBLG (**9**) via CuAAC between azido-functionalized C2TA-N_3 (**3**) or CTA-N_3 (**4**) and alkyne-functionalized PBLG (**7**). (The chemical structures of the N-termini of compounds **7**, **8**, and **9** are not exactly drawn; see "Materials and methods" section.)

DP = 19, $[M + Na]^+$ = 4,355.858; DP = 20, $[M + Na]^+$ = 4,575.410; DP = 21, $[M + Na]^+$ = 4,794.315; DP = 22, $[M + Na]^+$ = 5,013.887; DP = 23, $[M + Na]^+$ = 5,233.070; DP = 24, $[M + Na]^+$ = 5,453.077; carboxyl end group series (Cao et al. 2012), *m/z* DP = 14, $[M + H]^+$ = 3,388.627; DP = 15, $[M + H]^+$ = 3,608.965; DP = 16, $[M + H]^+$ = 3,827.815; DP = 17, $[M + H]^+$ = 4,047.109; DP = 18, $[M + H]^+$ = 4,266.354; DP = 19, $[M + H]^+$ = 4,485.536; DP = 20, $[M + H]^+$ = 4,703.741; DP = 21, $[M + H]^+$ = 4,923.701; DP = 22, $[M + H]^+$ = 5,143.429; DP = 23, $[M + H]^+$ = 5,362.840, 500 MHz ^{1}H-NMR ($CDCl_3$): δ 2.27 (Hβ), 2.60 (Hγ), 3.94 (Hα), 5.04 (OCH_2Ph), 7.2–7-4 (aromatic H); 125 MHz ^{13}C-NMR ($CDCl_3$): δ 25.5 (Cβ), 30.9 (Cγ), 56.8 (Cα), 66.1 (OCH_2Ph), 128.1, 128.5, 136.0 (aromatic C), 172.0 (Cδ=O), 175.3 (CαC=O); DSC: T_g = approx. 10 °C; T_{dec} = over 270 °C.

Synthesis of 2,3,4,6-tetra-*O*-acetyl-β-D-glucopyranosyl-(1 → 4)- 2,3,6-tri-*O*-acetyl-β-D-glucopyranosylazide-*block*-poly(γ-benzyl-L-glutamate) (8)

To a solution of 2,3,4,6-tetra-*O*-acetyl-β-D-glucopyranosyl-(1 → 4)-2,3,6-tri-*O*-acetyl-β-D-glucopyranosylazide (**3**, C2TA-N_3) (3.8 mg) and alkyne-functionalized poly(γ-benzyl-L-glutamate) (**7-1**, 22.6 mg, DP_n = 26.6) in anhydrous DMF (1.0 mL), *N,N,N′,N″,N‴*-pentamethyldiethylenetriamine (PMDETA) (16.0 μL), and an aqueous solution of sodium ascorbate (30.3 mg/38 μL) were added. The reaction mixture was degassed. Copper(I) bromide (11.0 mg) was then added to the reaction mixture. The reaction mixture was stirred under nitrogen atmosphere at r.t. for 27 h. The reaction product was concentrated to dryness. The crude product was washed with distilled water, and methanol to afford diblock copolymer **8** (19.7 mg, 78 % yield). MALDI-TOF MS analysis revealed that all the PBLG blocks feature pyroglutamate (Habraken et al. 2011) end groups. MALDI-TOF MS (positive linear mode, DHB used as a matrix) *m/z* DP = 6, $[M + Na]^+$ = 1,946.418; DP = 7, $[M + Na]^+$ = 2,165.414; DP = 8, $[M + Na]^+$ = 2,384.429; DP = 9, $[M + Na]^+$ = 2,603.416; DP = 10, $[M + Na]^+$ = 2,822.470; DP = 11, $[M + Na]^+$ = 3,041.134; DP = 12, $[M + Na]^+$ = 3,260.851; DP = 13, $[M + Na]^+$ = 3,480.163; DP = 14, $[M + Na]^+$ = 3,699.231; DP = 15, $[M + Na]^+$ = 3,918.447; DP = 16, $[M + Na]^+$ = 4,137.948; DP = 17, $[M + Na]^+$ = 4,356.637; DP = 18, $[M + Na]^+$ = 4,574.933; DP = 19, $[M + Na]^+$ = 4,795.813; DP = 20, $[M + Na]^+$ = 5,013.299;

Table 1 Synthesis of C2TA-*b*-PBLG (**6**) via ROP of BLG NCA (**5**)

Initiator	Comp. no.	Molecular weight				Diblock copolymer							
						Comp. no.	(Initiator)/(amino acid NCA)		Molecular weight				
		M_n	10^{-3} M_n	10^{-3} M_w	DP_n			Yield (%)	10^{-3} M_n	10^{-3} M_w	M_w/M_n	$DP_{n,\ GPC}$ of PBLG	$DP_{n,\ NMR}$ of PBLG
C2TA-NH_2	**1**	635.57	–	–	2	**6**[a]	1/15	70	2.7	5.2	2.0	9.2	59.4
CTA-NH_2	**2**	–	10	18	35.9	**–**	1/15	Trace	–	–	–	–	–

[a] Aggregation of diblock copolymers was observed. DP of oligopeptide blocks was estimated by GPC

DP = 21, $[M + Na]^+$ = 5,233.066; DP = 22, $[M + Na]^+$ = 5,452.221; DP = 23, $[M + Na]^+$ = 5,672.760. Number-averaged molecular weight (DP_n) of alkyne-functionalized PBLG calculated by ^{1}H-NMR measured in $CDCl_3$ with 15 % trifluoroacetic acid: 26.6; molecular weight in $CHCl_3$ was estimated by GPC. Number-averaged molecular weight: 1.9×10^3; weight-averaged molecular weight: 2.6×10^3, DP_n calculated by ^{1}H-NMR measured in $CDCl_3$: 53.8. 500 MHz ^{1}H-NMR ($CDCl_3$): δ 1.98–2.09 (CH_3CO), 2.28 (Hβ), 2.59 (Hγ), 3.92 (Hα), 5.03 (OCH_2Ph), 7.2–7.4 (aromatic protons), 8.33 (NH); 125 MHz ^{13}C-NMR ($CDCl_3$): δ 20.5 (CH_3CO), 25.6 (Cβ), 30.9 (Cγ), 56.8 (Cα), 66.2 (OCH_2Ph), 128.1, 128.5, 136.0 (aromatic C), 172.0 (Cδ=O), 175.4 (CαC=O). Note that the carbon resonances of the cellobiosyl residue were hidden in the baseline noise.

Synthesis of tri-*O*-acetyl cellulose-*block*-poly(γ-benzyl-L-glutamate) (9)

To a solution of tri-*O*-acetyl cellulosylazide (**4**, 50.1 mg, $DP_n = 41.6$) and alkyne-functionalized poly(γ-benzyl-L-glutamate) (**7-2**, 134.0 mg, DP_n = 47.1) in DMSO (3 mL), an aqueous solution of copper(II) sulfate pentahydrate (12 mg/50 μL) and an aqueous solution of sodium ascorbate (20.5 mg/50 μL) were added. The reaction mixture was stirred at r.t. for 21 h. The reaction mixture was added into a large excess of methanol, and the precipitate was collected by centrifugation (15,000 rpm, 10 min) to afford crude tri-*O*-acetyl cellulose-*block*-poly(γ-benzyl-L-glutamate) (159.2 mg). The crude CTA-*b*-PBLG was purified by gel filtration chromatography (LH-60, eluent: methanol/dichloromethane 1/4, v/v) to afford pure diblock copolymer CTA-*b*-PBLG (**9**) (84.3 mg, 85 % yield). Number-averaged degree of polymerization (DP_n) of the PBLG segment calculated by ^{1}H-NMR measured in $CDCl_3$: 68.8, based on the supposition that DP_n of the CTA segment is 41.6; molecular weight estimated by GPC: number-averaged molecular weight of **9**: 2.7×10^3; weight-averaged molecular weight of **9**: 9.5×10^3, 500 MHz ^{1}H-NMR ($CDCl_3$): δ 1.94, 2.01, 2.13 (CH_3CO), 2.26 (Hβ), 2.59 (Hγ), 3.55 (H5), 3.72 (t, $J = 8.5$, H4), 3.93 (Hα), 4.07 (d, $J = 7.0$, H6), 4.38 (d, $J = 10.5$, H6), 4.42 (d, $J = 7.0$, H1), 4.80 (t, $J = 8.0$, H2), 5.0–5.2 (H3 and OCH_2Ph), 7.2–7.4 (aromatic H), 8.01 (H at position 5 of 1,4-disubstituted 1,2,3-triazole); 125 MHz ^{13}C-NMR ($CDCl_3$): δ 20.4, 20.5, 20.8 (CH_3CO), 25.5 (Cβ), 30.8 (Cγ), 56.8 (Cα), 62.0 (C6), 66.1 (OCH_2Ph), 71.8 (C2), 72.5 (C3), 72.8 (C5), 76.0 (C4), 100.5 (C1), 128.1, 128.4, 136.0 (aromatic C), 169.3, 169.7, 170.2 (CH_3CO), 172.0 (Cδ=O), 175.4 (CαC=O); DSC: T_g of PBLG segment = approx. 10 °C; T_g of CTA segment = approx. 144 °C; T_c of CTA segment = 205 °C.

Atomic force microscopy (AFM), field emission scanning electron microscopy (FE-SEM) and transmission electron microscopy (TEM)

A few drops of a 0.1 wt% solution of CTA-*b*-PBLG (**9**) in dichloromethane were dropped, spin-coated at 1,000 rpm for 30 s, and dried on the surface of a silicon wafer. The obtained thin film of CTA-*b*-PBLG was dried under vacuum at r.t. for 6 days, and observed under an atomic force microscopy (SPM-9600, Shimadzu) in dynamic and phase modes. The thin film of CTA-*b*-PBLG was then annealed under vacuum at 180 °C for 24 h, and observed under an AFM in dynamic and phase modes. The cantilever probe (Olympus, OMCL-AC240TS-C2 or OMCL-AC200TS-C3) was used.

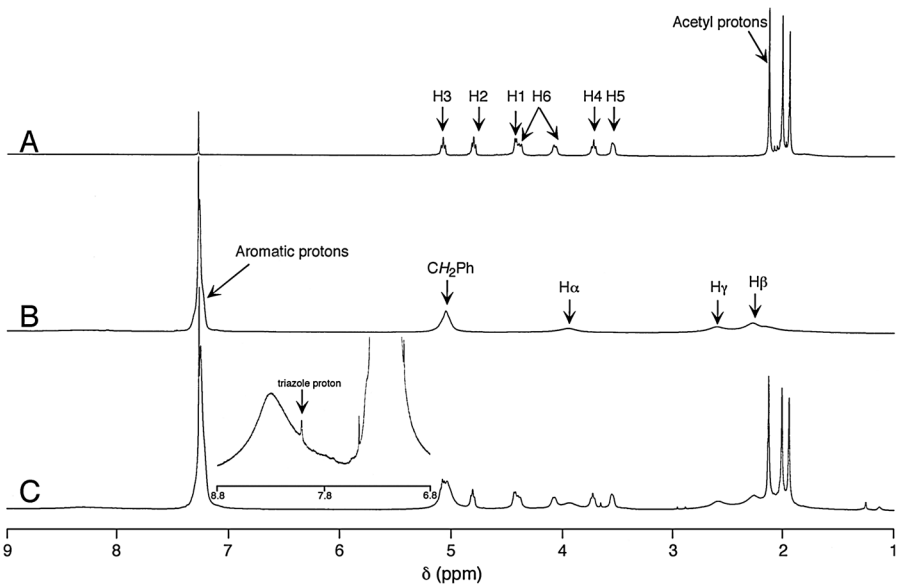

Fig. 1 ^{1}H NMR spectra of **A** azido-functionalized cellulose triacetate (**4**), **B** alkyne-functionalized PBLG (**7-2**), and **C** CTA-*b*-PBLG (**9**)

A few drops of a 0.1 wt% solution of CTA-*b*-PBLG (**9**) in chloroform were dropped and dried on the surface of a silicon wafer. The obtained thin film of CTA-*b*-PBLG was annealed at 180 °C for 24 h and stained overnight by the vapor of a 0.5 % aq. RuO_4 solution at room temperature. The surface of the film was observed under a field emission scanning electron microscope (S-4800; Hitachi) at an accelerating voltage of 1.5 kV and a 2.5 mm working distance. To visualize the distribution of ruthenium, a back-scattered electron microscopy (BSE) signal was obtained. For better comparison with the TEM images, the BSE signal was inverted.

A block of CTA-*b*-PBLG (**9**) was annealed at 180 °C for 24 h, stained by the vapor of a 0.5 % aq. RuO_4 solution for 24 h at room temperature, and then embedded in epoxy resin. Ultrathin sections were obtained from the epoxy resin-embedded blocks using an ultramicrotome equipped with a diamond knife. The sections were mounted on copper grids with an elastic carbon supporting film (Oken Shoji, Japan) and observed under a transmission electron microscope (JEM1400; JEOL) at an accelerating voltage of 100 kV. It is known that ruthenium tetroxide readily stains many polymers (Trent et al. 1983) and compounds containing double bonds (Howell and Reneker 1990). It is likely that the PBLG block is stained more readily than the CTA block (de Oliveira and Glasser 1994).

Results and discussion

Two strategies

We explored two methods of preparing cellulosic diblock copolymers, as shown in Scheme 1. Anionic ring-opening polymerization (ROP) of BLG NCA (**5**) initiated from cellulose triacetate derivatives as macroinitiators would provide CTA-*b*-PBLG. The second strategy involves a coupling reaction, CuAAC, between azido end-functionalized tri-*O*-acetyl-cellulosylazide (**4**) and alkyne end-functionalized PBLG (**7**). We compared the efficiency of those reactions in producing cellulosic diblock copolymers.

Synthesis of C2TA-*b*-PBLG (6) via ROP of BLG NCA (5)

The reactivity of the macroinitiator, CTA-NH_2 (**2**), for the ROP of BLG NCA (**5**) remains unknown. C2TA-NH_2 (**1**) was therefore selected as a model polymeric cellulose derivative for the ROP initiation reaction of BLG NCA (**5**). The reactivities of the amino groups at the ends of CTA-NH_2 (**2**) and C2TA-NH_2 (**1**) were compared.

Table 1 summarizes the results of the ROP of BLG NCA (**5**) to afford cellulosic diblock copolymers. C2TA-NH_2 (**1**) was able to initiate the ROP of BLG NCA (**5**) to afford C2TA-*b*-PBLG (**6**) with a DP_n of

Table 2 Synthesis of C2TA-*b*-PBLG (**8**) and CTA-*b*-PBLG (**9**) via CuAAC

	Comp. no.	Cellulosic segment				PBLG (**7**)						Diblock copolymer							
		Molecular weight				Comp. no.	Molecular weight					Comp. no.	(Azide)/(alkyne)	Yield		Molecular weight			
		M_n	10^{-3} M_n	10^{-3} M_w	DP_n		10^{-3} M_n	10^{-3} M_w	M_w/M_n	$DP_{n,\ GPC}$	$DP_{n,\ NMR}$			Solv.	(%)	10^{-3} M_n	10^{-3} M_w	M_w/M_n	$DP_{n,\ GPC}$ of PBLG	$DP_{n,\ NMR}$ of PBLG
C2TA-N_3	**3**	661.57	–	–	2	**7-1**	0.38	0.52	1.4	1.5	26.6	**8**[a]	1/1.5	DMF	78	1.9	2.6	1.3	5.5	53.8
CTA-N_3	**4**	–	12.1	24.1	41.6	**7-2**	2.2	3.4	1.6	9.8	47.1	**9**	1/2.75	DMSO	85	2.7	9.5	3.6	–	68.8[b]

[a] Molecular weight of a molecularly dispersed part in $CHCl_3$ was estimated by GPC

[b] DP_n of PBLG of CTA-b-PBLG was calculated based on the supposition that DPn of CTA is 41.6

PBLG of 59.4, as calculated from a comparison of the proton resonance area of C2TA with that of PBLG in its ^{1}H-NMR spectrum (see Supporting Information, Figure S1). GPC analysis indicated a DP_n of PBLG of 9.2, which is smaller than that calculated by ^{1}H-NMR, likely because C2TA-*b*-PBLG (**6**) aggregates in chloroform and part of polymer, including the PBLG segment, was probably removed when filtering the solution (pore size: 2.7 μm) or by the guard column. The NMR measurement of **6** in $CDCl_3$ afforded a convincing DP_n 59.4. In contrast, CTA-NH_2 (**2**) did not initiate the ROP of BLG NCA (**5**). We concluded that either the amino functional group at the end of tri-*O*-acetyl cellulose is not sufficiently nucleophilic to initiate the ROP of PBLG or the bulkiness of the CTA segment disturbs the ROP initiation process. We therefore investigated a second strategy, using Cu-AAC, to reach the cellulosic diblock copolymer CTA-*b*-PBLG.

Synthesis of C2TA-*b*-PBLG (8) and CTA-*b*-PBLG (9) via copper-catalyzed azide–alkyne cycloaddition (CuAAC) between azido-functionalized C2TA-N_3 (3)/CTA-N_3 (4) and alkyne-functionalized PBLG (7)

Proton NMR experiments of PBLGs (**7-1**) and (**7-2**) measured in $CDCl_3$ containing 15 % TFA revealed that the DP_ns of alkyne-functionalized PBLGs (**7-1**) and (**7-2**) were 26.6 and 47.1, respectively (See Supporting Information: the ^{1}H-NMR spectra of compounds **7-1** and **7-2** are shown in Figures S2 and S4, respectively).

To confirm the reactivity of CuAAC, azido-functionalized C2TA-N_3 (**3**), as a model cellulose derivative with low molecular weight, was coupled with alkyne-functionalized PBLG (**7-1**), resulting in the synthesis of diblock copolymer C2TA-*b*-PBLG (**8**) with a DP_n of PBLG 53.8, as confirmed by ^{1}H-NMR measurements in $CDCl_3$ (see Supporting Information: the ^{1}H-NMR spectrum of compound **8** is shown in Figure S3). The molecular weight of compound **8** was also underestimated by GPC analysis (chloroform as an eluent) likely because C2TA-*b*-PBLG (**8**) aggregates in chloroform and part of polymer, including the PBLG segment, was probably removed when filtering the solution (pore size: 2.7 μm) or by the guard column. Contrary to the low reactivity of CTA-NH_2 (**2**) as a macroinitiator for the ROP of BLG NCA (**5**),

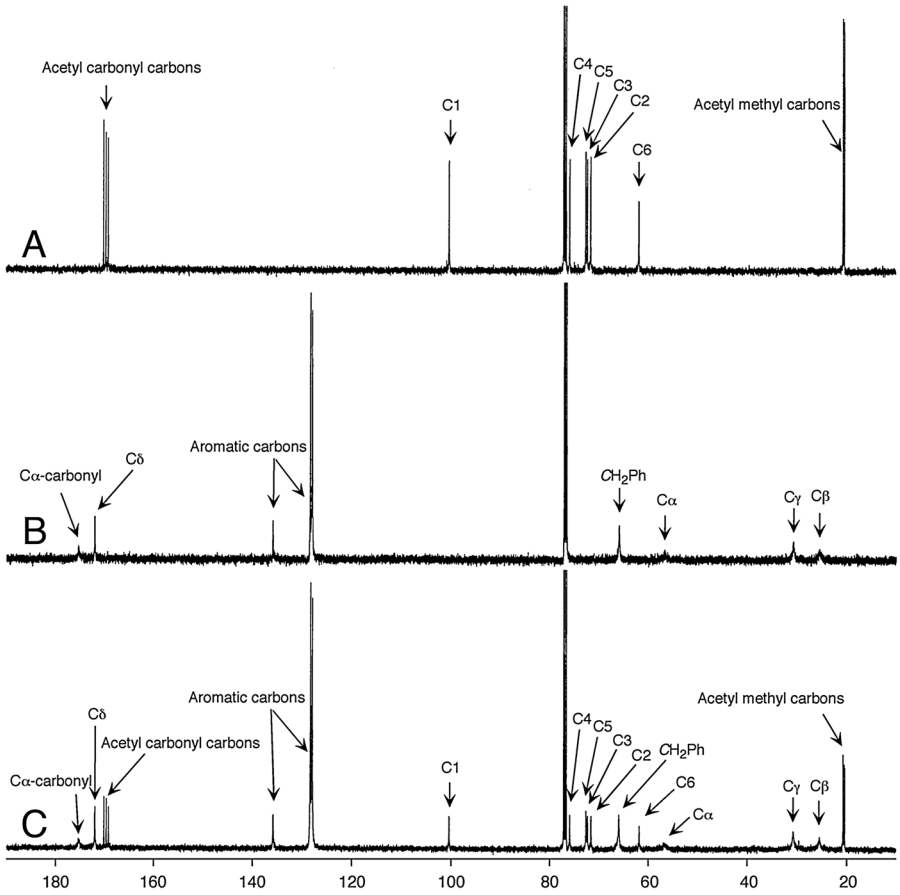

Fig. 2 ^{13}C NMR spectra of **A** azido-functionalized cellulose triacetate (**4**), **B** alkyne-functionalized PBLG (**7-2**), and **C** CTA-*b*-PBLG (**9**)

the azido group at the end of CTA showed a relatively high reactivity, and CuAAC between CTA-N_3 (**4**) and PBLG (**7-2**) proceeded successfully to produce CTA-*b*-PBLG (**9**). Because the GPC analysis of the diblock copolymer (**9**) exhibited a smaller molecular weight compared to the starting CTA-N_3 (**4**), we were unable to evaluate the DPs of both the CTA and PBLG segments of the resulting diblock copolymer CTA-*b*-PBLG (**9**). The hydrodynamic diameter of the alkyne-functionalized PBLG gradually increased with increasing time after its dissolution in $CHCl_3$, indicating that PBLG gradually aggregated in $CHCl_3$, as confirmed by dynamic light scattering experiments (data not shown). During GPC analysis, part of polymer, including the PBLG segment, was probably removed when filtering the solution (pore size: 0.45 μm) or by the guard column. Proton NMR analysis afforded a reasonable DP_n value for PBLG of 68.8 of CTA-*b*-PBLG (**9**), which was calculated based on the supposition that the DP_n of the CTA segment in CTA-*b*-PBLG (**9**) is 41.6.

Structure determination of CTA-*b*-PBLG (**9**)

Figure 1 shows the ^1H-NMR spectra of (A) azido end-functionalized CTA (**4**), (B) alkyne end-functionalized PBLG (**7-2**), and (C) CTA-*b*-PBLG (**9**) measured in $CDCl_3$. All protons of CTA-N_3 (**4**) were assigned as shown in Fig. 1a. The anomeric proton at the reducing-end of CTA-N_3 (**4**) appears at 4.60 ppm as a trace of a doublet ($J = 9.0$ Hz). Figure 1b shows broad proton resonances appearing at 3.94, 2.27, and 2.60 ppm, which were assigned to Hα, Hβ, and Hγ of the alkyne-functionalized PBLG (**7-2**), respectively. Although the protons resonances of the propargyl residues overlapped with those of the PBLG residues or could not be measured in $CDCl_3$ due to the aggregation of PBLG in chloroform, the methylene protons of the propargyl residue readily appear at 3.95 ppm (Wang et al. 2008) in a ^1H-NMR spectrum of propargyl-terminated PBLG (**7-2**) recorded in $CDCl_3$ containing 15 % TFA (Agut et al. 2008) (See Supporting Information: the ^1H-NMR spectrum of

compound **7-2** is shown in Figure S4). Using the NMR spectrum, we calculated the number-averaged degree of polymerization (DP_n) of the alkyne end-functionalized PBLG (**7**) as shown in Table 2. In Fig. 1c, the proton resonances of the CTA and PBLG segments of the diblock copolymer CTA-*b*-PBLG (**9**) appear as relatively broad signals. A weak resonance assigned to a proton at position 5 of a 1,4-disubstituted 1,2,3-triazole product appeared at 8.01 ppm as a singlet, indicating that CuAAC between azido-functionalized CTA (**4**) and alkyne-functionalized PBLG (**7-2**) proceeded successfully.

Figure 2 shows the ^{13}C-NMR spectra of (A) azido end-functionalized CTA (**4**), (B) alkyne end-functionalized PBLG (**7-2**), and (C) CTA-*b*-PBLG (**9**) measured in $CDCl_3$. The carbon resonance of C1 at the reducing end of the CTA residue could not be assigned, though all the protons of the CTA internal residues appeared, as shown in Fig. 2a. The Cβ, Cγ, and Cα carbons, as well as the two carbonyl carbons Cδ=O and Cα-C=O of alkyne end-functionalized PBLG (**7-2**), appeared at 25.5, 30.9, 56.8, 172.0, and 175.3 ppm, respectively, although the carbon resonances of the propargyl end group could not be found. MALDI-TOF MS analysis of the alkyne end-functionalized PBLG (**7-2**) confirmed that propargylamine initiated the ROP of PBLG. As shown in Fig. 2c, the internal residues of both the CTA and PBLG segments appeared and were assigned.

Figure 3 shows the infrared spectra of (A) tri-*O*-acetylcellulosylazide (**4**), (B) alkyne-functionalized PBLG (**7-2**), and (C) CTA-*b*-PBLG (**9**). Although the absorption of the azido group appeared at 2,120 cm^{-1} in spectrum (A), no absorption band was observed at the same wavenumber in spectrum (C). This means

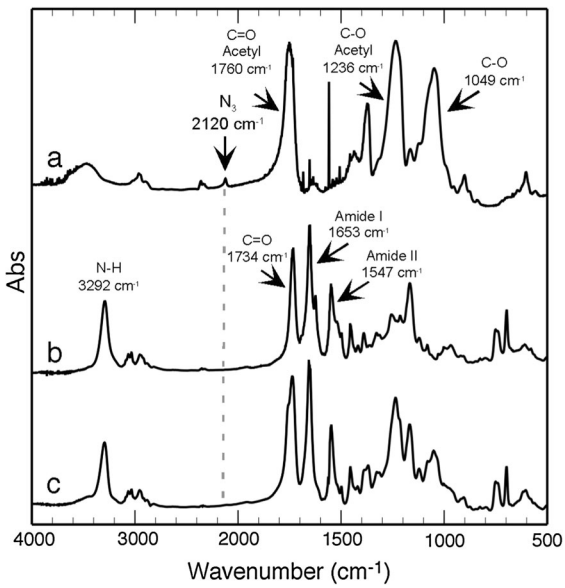

Fig. 3 Infrared spectra of **a** azido-functionalized cellulose triacetate (**4**), **b** alkyne-functionalized PBLG (**7-2**), and **c** CTA-*b*-PBLG (**9**)

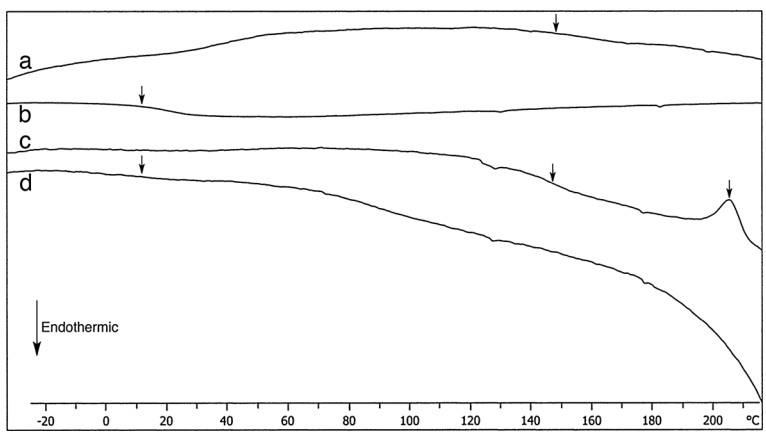

Fig. 4 Differential scanning calorimetry thermograms of **a** azido-functionalized cellulose triacetate (**4**) (2nd heating scan up to 290 °C), **b** alkyne-functionalized PBLG (**7-2**) (1st heating scan up to 290 °C after three heating scans up to 210 °C), **c** CTA-*b*-PBLG (**9**) (2nd heating scan up to 290 °C after three heating scans up to 210 °C and one heating scan up to 290 °C), and **d** CTA-*b*-PBLG (**9**) (1st heating scan up to 290 °C after three heating scans up to 210 °C). Heating rate: 5 °C/min; cooling rate: −50 °C/min; heating cycle: −40 to 210 °C three times, then −40 to 290 °C three times

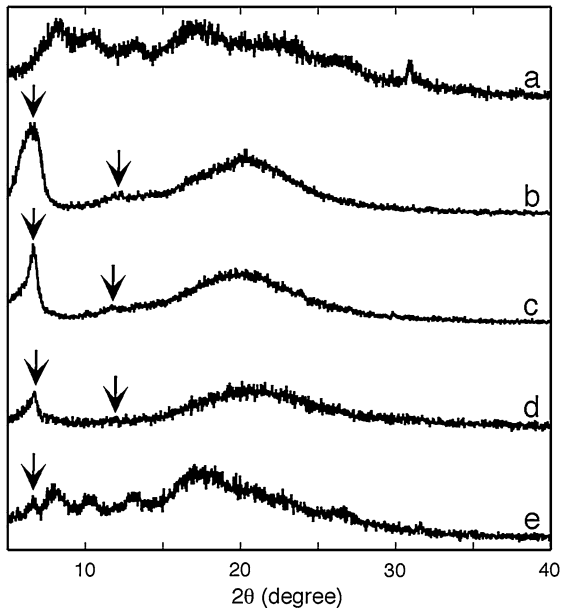

Fig. 5 Wide angle X-ray diffractograms of **a** azido-functionalized cellulose triacetate (**4**) with a CTA-II crystal structure before annealing, **b** alkyne-functionalized PBLG (**7-2**) before annealing, **c** PBLG (**7-2**) after annealing at 180 °C for 24 h, **d** CTA-*b*-PBLG (**9**) before annealing, and **e** CTA-*b*-PBLG (**9**) after annealing at 180 °C for 24 h

that CuAAC proceeded completely and that no CTA-N_3 (**4**) remained after the purification process.

The amide I and II bands appeared at 1,653 and 1,547 cm^{-1}, respectively, both in spectra b and c. The IR spectrum (c) shows that CTA-*b*-PBLG (**9**) contains both CTA and PBLG segments. The characteristic absorption band of the C=O group at 1,734 cm^{-1} and that of the acetyl carbonyl group at 1,760 cm^{-1} overlap in the spectrum of CTA-*b*-PBLG (**9**). The amide I band at 1,653 cm^{-1} indicates that PBLG exhibits an α-helix structure (Miyazawa 1960; Chirgadze and Brazhnikov 1974; Chirgadze et al. 1976; Lopez-Carrasquero et al. 1995) before annealing over the T_g of CTA, as described later.

Crystallization-induced microphase separation of CTA-*b*-PBLG (**9**)

Figure 4 shows the DSC curves of (a) azido-functionalized CTA (**4**), (b) alkyne-functionalized PBLG (**7-2**), and (c) and (d) CTA-*b*-PBLG (**9**). The glass transition temperatures (T_g) of CTA-N_3 (**4**) appeared at 144 °C, as shown in curve (a). The T_g of CTA with a low DP is known to appear at relatively low temperature (Kamitakahara et al. 2005). As shown in curve (b), T_g of the alkyne-functionalized PBLG (**7-2**) appeared at approx. 10 °C, which is comparable to previously reported values (Mckinnon and Tobolsky 1966; Koleske and Lundberg 1969; Watanabe and Uematsu 1984; Papadopoulos et al. 2004). In contrast, the T_gs of both the CTA and PBLG blocks appeared in diblock copolymer CTA-*b*-PBLG (**9**) in curves (c) and (d), respectively. Part of the alkyne-functionalized PBLG (**7-2**) presumably decomposed over 270 °C, because a large endothermic peak appeared in a first heating scan up to 290 °C. CTA-N_3 (**4**) showed a melting temperature (T_m) at 296 °C (heating rate: 10 °C/min), and an endothermic peak was observed from approx. 270 to 300 °C. Powders of CTA-N_3 (**4**), probably containing both amorphous phase and CTA-II crystals, were used for the DSC measurements, with the result being that T_g of CTA-N_3 (**4**) was not clearly observed in heating scans up to 210 °C, and then appeared in curve (a) after heating up to 290 °C, which is near the melting temperature of CTA-N_3 (**4**). Two separate T_gs of the CTA and PBLG blocks in the diblock copolymer CTA-*b*-PBLG (**9**) in one heating curve were unable to be observed, because the T_m of the CTA block is higher than or close to the decomposition temperature of the PBLG block. In addition, the cold crystallization temperature (T_c) of CTA-*b*-PBLG (**9**) was observed in a 2nd heating curve of CTA-*b*-PBLG (**9**) (c) at 205 °C. These facts indicate that the CTA and PBLG segments exist separately in the bulk.

The DSC data suggested that thermal treatment would enhance the microphase separation of CTA-*b*-PBLG (**9**). We therefore investigated the crystal structures of CTA-N_3 (**4**) and alkyne-functionalized PBLG (**7-2**) homopolymers and CTA-*b*-PBLG diblock copolymer (**9**) before and after annealing at 180 °C, which is higher than the T_g of CTA-*b*-PBLG (**9**), for 24 h by WAXD experiments. Figure 5 shows the WAXD profiles of CTA (**4**), PBLG (**7-2**), and CTA-*b*-PBLG (**9**). Figure 5a indicates that CTA has the CTA-II crystal structure even before annealing. PBLG exhibited an α-helix structure, as demonstrated by the appearance of diffractions (d = 13.4 Å and 7.4 Å: see arrows in Fig. 5b). Bragg reflections were found at scattering vectors with a ratio of $1:3^{1/2}$ at $2\theta = 6.62°$ (13.4 Å) and 11.2° (7.4 Å), indicating a

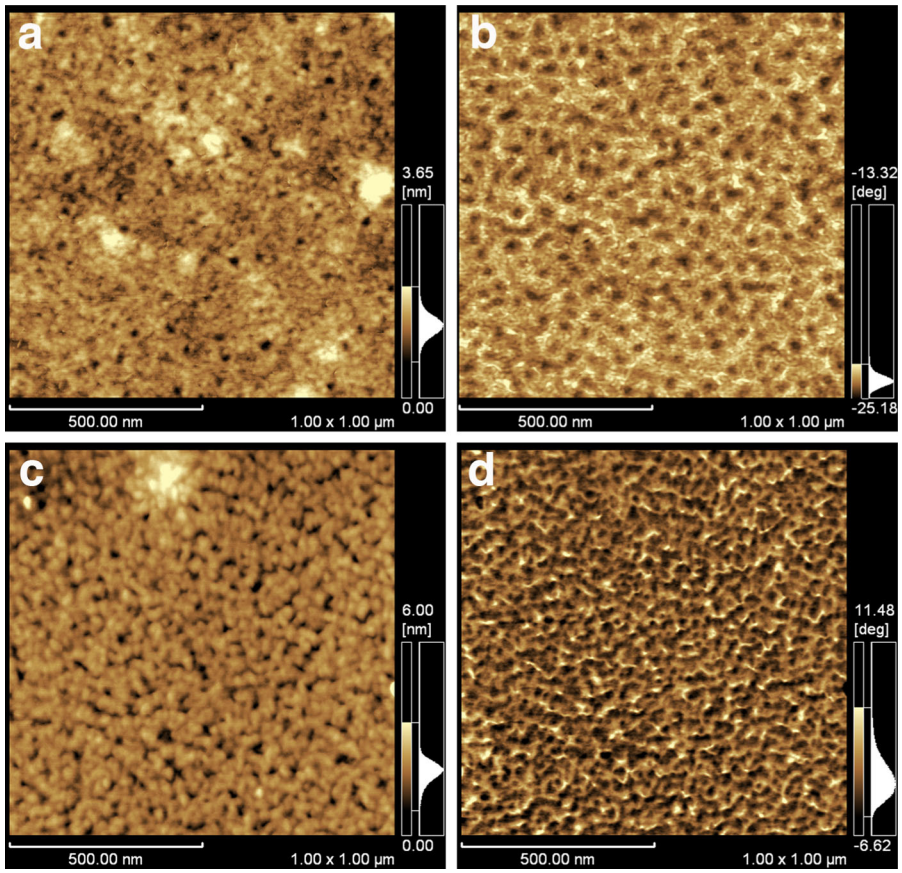

Fig. 6 Atomic force microscopy images of a CTA-*b*-PBLG thin film. Topographic images **a** before and **c** after annealing, respectively, and phase images **b** before and **d** after annealing, respectively

hexagonal columnar arrangement and 18/5 α-helical conformation of PBLG with a columnar diameter of 1.35 nm (Floudas et al. 2003; Zhou et al. 2010). After annealing, the crystallinity of the α-helix structure in PBLG (**7-2**) increased, as shown in Fig. 5c. In contrast, although an 18/5 α-helix structure of CTA-*b*-PBLG (**9**) appeared, no crystal structure was found in the CTA segment before annealing, as shown in Fig. 5d. The CTA-II crystal structure of the CTA segment in CTA-*b*-PBLG (**9**) appeared after annealing at 180 °C for 24 h as along with the α-helix structure of the PBLG segment, though the crystallinity of PBLG decreased. This phenomenon means that the CTA block separately crystallized in the bulk CTA-*b*-PBLG (**9**), causing the decrease in the α-helix structure in PBLG; it also strongly suggests that the thermal treatment, namely, the crystallization of CTA, enhanced the microphase separation between the CTA and PBLG segments at the molecular level, as described later.

Microphase separation of CTA-*b*-PBLG (9) as observed by AFM, FE-SEM and TEM

Oligopeptides of γ-benzyl-L-glutamate are known to form two secondary structures: α helices and β sheets stabilized by intra- and intermolecular hydrogen bonds, respectively (Papadopoulos et al. 2004). PBLG normally exhibits an α helix with an 18/5 helical conformation and a 0.54 nm spiral pitch, 3.6 residues per turn, affording 18 residues in five turns (Watanabe and Uematsu 1984). DP_n of the PBLG block of CTA-*b*-PBLG (**9**) was estimated as 68.8 by ^{1}H-NMR analysis. The length of the PBLG block was therefore calculated as $68.8/3.6 \times 0.54 = 10.3$ nm.

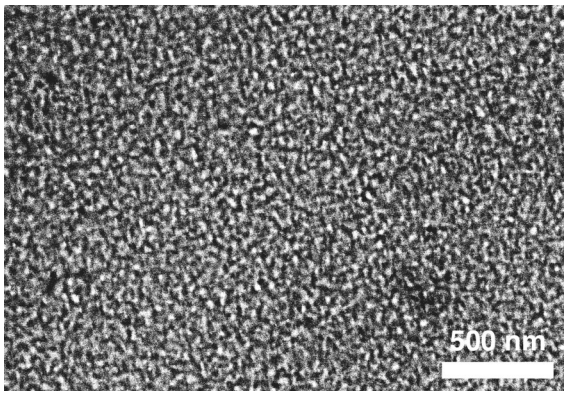

Fig. 7 Field emission scanning microscopy image by back scattering electron of a CTA-*b*-PBLG thin film, stained by ruthenium tetroxide. The color of the image was inverted for easy understanding of the image, comparable to those shown in Fig. 8. The image clearly shows the microphase separation of the dark parts (PBLG segments) and the bright layer (CTA segments)

Atomic force microscopy images of the thin film of CTA-*b*-PBLG are shown in Fig. 6. Both topographic and phase images changed after annealing at 180 °C for 24 h. In the phase image (b) before annealing, ellipsoidal particles with dimensions of about 15 nm for the semi-major axis and of circa 8 nm for the semi-minor one were detected. Those particles likely tend to orient in parallel. After the annealing process, both topological (c) and phase (d) images indicate that the film of CTA-*b*-PBLG (**9**) exhibits microphase separation. This fact is consistent with FE-SEM and TEM images of CTA-*b*-PBLG (**9**), as described later.

An inverted BSE image of the thin film of CTA-*b*-PBLG stained by RuO_4 vapor taken by FE-SEM is shown in Fig. 7. The image clearly indicates that the film of CTA-*b*-PBLG (**9**) exhibits microphase separation, and the dark parts stained by RuO_4 are likely PBLG segments. RuO_4 did not stain the CTA segments. The molecular length of $CTA_{41.6}$-*b*-$PBLG_{68.8}$ (**9**) was calculated as ca. 32.2 nm (21.9 nm (CTA) + 10.3 nm (PBLG α-helix)). The average thicknesses of the bright layer, CTA, and the dark layer, PBLG, were approx. 31 and 14 nm, respectively. The experimental data from FE-SEM is, therefore, likely consistent with the fact that the X-ray diffractogram of CTA-*b*-PBLG (**9**) displayed a CTA-II crystal structure, indicating anti-parallel packing of the CTA segments. The CTA segments

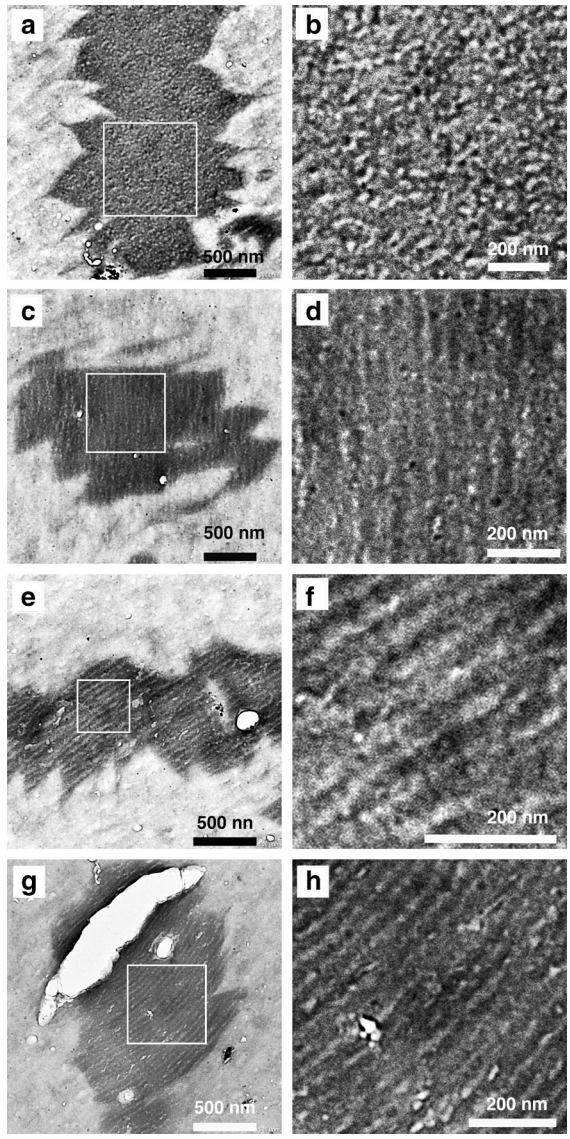

Fig. 8 Transmission electron microscopy images taken from ultrathin sections of CTA-*b*-PBLG (**9**) stained by ruthenium tetroxide vapor. Images **b**, **d**, **f**, and **h** are enlarged images from the square regions in **a**, **c**, **e**, and **g**, respectively. Microphase separation of the dark parts (PBLG segments) and bright layers (CTA segments) can be seen in different directions of ultrathin sectioning

probably interpenetrate or interdigitate in an anti-parallel direction to form bright ellipsoidal parts. The PBLG segments possibly produce double layers or an interpenetrated single layer of α-helices or random coils to afford the 14 nm thick dark part.

Transmission electron microscopy images of ultrathin sections of CTA-*b*-PBLG (**9**) are shown in Fig. 8.

Part of the bulk CTA-*b*-PBLG bulk was stained by RuO_4 vapor, likely because RuO_4 vapor was able to pass through holes in the diblock polymer bulk, and the polymers around the holes were preferentially stained. Microphase separation of the dark parts (PBLG segments) and bright layer (CTA segments) can be seen in different directions of the ultrathin sectioning (Fig. 8a, c, e, g). The morphologies of CTA-*b*-PBLG (**9**) shown in Fig. 8a, b are similar to those seen in the FE-SEM image in Fig. 7. In addition, characteristic lamellar-like morphologies were observed in Fig. 8c–h.

Bulk lamellar morphologies, including hexagon in lamella (HL) structure, have been investigated for peptide-containing copolymers as well (Papadopoulos et al. 2005; Sanchez-Ferrer and Mezzenga 2010). However, the present CTA-*b*-PBLG (**9**) formed different self-organization patterns. Thermal treatment over the T_g of CTA destroyed the hexagonal packing of PBLG, as demonstrated by the wide angle X-ray diffractograms, and preferentially induced CTA-crystallization-driven microphase separation. CTA possesses a CTA II crystal structure (space group: $P2_12_12_1$; dimensions $a = 24.68$ Å, $b = 11.52$ Å, and c (fiber axis) $= 10.54$ Å) (Roche et al. 1978; Dulmage 1957), and the distance between two CTA chains is shorter than that between two α helices of PBLG, probably resulting in the formation of a nearly amorphous structure of PBLG after annealing at 180 °C.

The nearly cylindrical (partly branched) morphology of the CTA portion is oriented nearly parallel in the polymer bulk, as shown in Figures c–h. A nearly spherical or partly ellipsoidal morphology of CTA-*b*-PBLG appears, as depicted in Fig. 8a, b, when the ultrathin section was sliced perpendicular to the direction of the cylindrical, partly branched CTA portion. The width of the bright and dark layers varies with the cutting angle to the direction of the cylindrical, partly branched CTA portion. The sizes of the bright and dark areas observed by TEM and FE-SEM were comparable.

Conclusions

We succeeded in the synthesis of well-defined CTA-*b*-PBLG via CuAAC, and we made the first observation of microphase separation of cellulosic materials in thin film and in bulk. The well-defined chemical structure of CTA-*b*-PBLG allowed us to build nanostructures of academic and practical interests. The crystallization-induced microphase separation by thermal treatment was key to produce the well-ordered nanostructure of the cellulosic diblock copolymer, CTA-*b*-PBLG. A more detailed investigation on the nanostructure of CTA-*b*-PBLG is of interest, and the preparation of CTA-*b*-PBLG with different lengths of the two segments will afford fundamental knowledge regarding the self-assembly of cellulosic diblock copolymers. This potent strategy for the preparation of microphase-separated cellulosic materials opens the door to new and valuable fields for cellulose such as medical applications and separation technologies. Moreover, our synthesis strategy is applicable to a wide range of cellulose esters such as cellulose diacetate (CDA) and cellulose ethers (Nakagawa et al. 2012), thereby producing diverse cellulosic diblock copolymers.

Acknowledgments We are indebted to Prof. Yoshiyuki Nishio of Kyoto University for the discussion on thermal analysis. We thank the Japan Society for the Promotion of Science (JSPS) for their financial support of this study, in part, through Grant-in-Aid for Scientific Research (nos. 21580205 and 24380092), and a Sekisui Chemical Grant Program for Research.

References

Agut W, Agnaou R, Lecommandoux S, Taton D (2008) Synthesis of block copolypeptides by click chemistry. Macromol Rapid Commun 29:1147–1155. doi:10.1002/Marc.200800123

Ando I, Yamada S, Sanefuji T, Shoji A, Uematsu I (1987) Effect of pressure on the molecular motion of a poly(γ-benzyl L-glutamate) lyotropic liquid crystal as studied by proton nuclear magnetic resonance. Polymer 28:716–720. doi:10.1016/0032-3861(87)90218-7

Caillol S, Lecommandoux S, Mingotaud A-F, Schappacher M, Soum A, Bryson N, Meyrueix R (2003) Synthesis and self-assembly properties of peptide-polylactide block copolymers. Macromolecules 36:1118–1124. doi:10.1021/ma021187c

Cao H, Yao J, Shao Z (2012) Synthesis of poly(γ-benzyl-L-glutamate) with well-defined terminal structures and its block polypeptides with alanine, leucine and phenylalanine. Polym Int 61:774–779. doi:10.1002/pi.4138

Ceresa RJ (1961) The synthesis of block and graft copolymer of cellulose and its derivatives. Polymer 2:213–219

Chen D (2013) Crystal behavior of semicrystalline polystyrene-block-poly(L-lactide) diblock copolymer in thin films with various structures. Polym Int 62:1343–1350. doi:10.1002/pi.4426

Chirgadze YN, Brazhnikov EV (1974) Intensities and other spectral parameters of infrared amide bands of polypeptides in the α-helical form. Biopolymers 13:1701–1712. doi:10.1002/bip.1974.360130902

Chirgadze YN, Brazhnikov EV, Nevskaya NA (1976) Intramolecular distortion of the α-helical structure of polypeptides. J Mol Biol 102:781–792. doi:10.1016/0022-2836(76)90291-6

Daly WH, Poche D (1988) The preparation of N-Carboxyanhydrides of alpha-amino-acids using bis(trichloromethyl)carbonate. Tetrahedron Lett 29:5859–5862. doi:10.1016/S0040-4039(00)82209-1

de Oliveira W, Glasser WG (1994) Multiphase materials with lignin 13. Block-copolymers with cellulose propionate. Polymer 35:1977–1985

Dulmage WJ (1957) The molecular and crystal structure of cellulose triacetate. J Polym Sci 26:277–288. doi:10.1002/Pol.1957.1202611402

Edgar KJ, Buchanan CM, Debenham JS, Rundquist PA, Seiler BD, Shelton MC, Tindall D (2001) Advances in cellulose ester performance and application. Prog Polym Sci 26:1605–1688. doi:10.1016/S0079-6700(01)00027-2

Enomoto Y, Kamitakahara H, Takano T, Nakatsubo F (2006) Synthesis of diblock copolymers with cellulose derivatives. 3. Cellulose derivatives carrying a single pyrene group at the reducing-end and fluorescent studies of their self-assembly systems in aqueous NaOH solutions. Cellulose 13:437–448

Enomoto-Rogers Y, Kamitakahara H, Yoshinaga A, Takano T (2011) Synthesis of diblock copolymers with cellulose derivatives 4. Self-assembled nanoparticles of amphiphilic cellulose derivatives carrying a single pyrene group at the reducing-end. Cellulose 18:1005–1014. doi:10.1007/S10570-011-9549-4

Farrar D, Yu MS, West JE, Moon W (2010) Piezoelectric biopolymer-polymer composite films and microfibers. Johns Hopkins APL Tech Dig 28:258–259

Feger C, Cantow HJ (1980) Cellulose containing block copolymers 1. Synthesis of trimethylcellulose-(b-poly(oxytetramethylene))-star block copolymers. Polym Bull 3:407–413

Floudas G, Papadopoulos P, Klok HA, Vandermeulen GWM, Rodriguez-Hernandez J (2003) Hierarchical self-assembly of poly(gamma-benzyl-L-glutamate)-poly(ethylene glycol)-poly(gamma-benzyl-L-glutamate) rod-coil-rod triblock copolymers. Macromolecules 36:3673–3683. doi:10.1021/Ma025918k

Habraken GJM, Wilsens KHRM, Koning CE, Heise A (2011) Optimization of N-carboxyanhydride (NCA) polymerization by variation of reaction temperature and pressure. Polym Chem 2:1322–1330. doi:10.1039/C1py00079a

Hiratsuka N, Shiba K, Shinomura K, Hosaki S, Cho H, Nagasaki A, Kobayashi S (1994) Urinary protein-fractions in healthy-subjects using cellulose-acetate membrane electrophoresis followed by staining with acid-violet-17. Biol Pharm Bull 17:1355–1357

Howell B, Reneker DH (1990) Morphology of polymer-films and single molecules. J Appl Polym Sci 40:1663–1682. doi:10.1002/App.1990.070400921

Ibarboure E, Papon E, Rodriguez-Hernandez J (2007) Nanostructured thermotropic PBLG–PDMS–PBLG block copolymers. Polymer 48:3717–3725. doi:10.1016/j.polymer.2007.04.046

Jadage CD, Lonikar SV, Wadgaonkar PP (2004) Starch and cellulose based graft and block copolymers. In: Society for polymer science, India, pp PD.1/1–PD.1/5

Kadokawa J-I, Karasu M, Tagaya H, Chiba K (1996) Synthesis of a block copolymer consisting of oligocellulose and oligochitin. J Macromol Sci, Pure Appl Chem A33:1735–1743. doi:10.1080/10601329608010937

Kamatani A, Kikuchi Y (2002) Carbohydrate diblock and triblock copolymers with desirable molecular weights and their manufacture. JP2002146025A,

Kamitakahara H, Nakatsubo F (2005) Synthesis of diblock copolymers with cellulose derivatives. 1. Model study with azidoalkyl carboxylic acid and cellobiosylamine derivative. Cellulose 12:209–219

Kamitakahara H, Enomoto Y, Hasegawa C, Nakatsubo F (2005) Synthesis of diblock copolymers with cellulose derivatives. 2. Characterization and thermal properties of cellulose triacetate-block-oligoamide-15. Cellulose 12:527–541

Kang IK, Ito Y, Sisido M, Imanishi Y (1988) Gas permeability of the film of block and graft copolymers of polydimethylsiloxane and poly(gamma-benzyl L-glutamate). Biomaterials 9:349–355

Kim S, Stannett VT, Gilbert RD (1973) A new class of biodegradable polymers. J Polym Sci Polym Lett 11:731–735

Kim S, Stannett VT, Gilbert RD (1976) Biodegradable cellulose block copolymers. J Macromol Sci Pt A Chem A10:671–679

Koleske JV, Lundberg RD (1969) Secondary transitions in poly(γ-benzyl-L-glutamate) and in poly(γ-benzyl-DL-glutamate). Macromolecules 2:438–440. doi:10.1021/ma60010a024

Kubota R, Machii R, Hiratsuka N, Hotta O, Itoh Y, Kobayashi S, Shiba K (2003) Cellulose acetate membrane electrophoresis in the analysis of urinary proteins in patients with tubulointerstitial nephritis. J Clinic Lab Anal 17:44–51. doi:10.1002/Jcla.10066

Lonikar SV, Gilbert RD, Fornes RE, Stejskal E (1990) Block copolymers of polysaccharides and polyamino acids. Abstracts of papers of the American Chemical Society 199:364-POLY

Lopez-Carrasquero F, Aleman C, Munoz-Guerra S (1995) Conformational analysis of helical poly(β-L-aspartate)s by IR dichroism. Biopolymers 36:263–271

Machii R, Kubota R, Hiratsuka N, Sugimoto K, Masudo R, Kurihara Y, Kobayashi S, Shiba K (2004) Urinary protein fraction in healthy subjects using cellulose acetate membrane electrophoresis followed by colloidal silver staining. J Clinic Lab Anal 18:231–236. doi:10.1002/Jcla.20028

Machii R, Sakatume M, Kubota R, Kobayashi S, Gejyo F, Shiba K (2005) Examination of the molecular diversity of alpha(1) antitrypsin in urine: deficit of an alpha(1) globulin fraction on cellulose acetate membrane electrophoresis. J Clinic Lab Anal 19:16–21. doi:10.1002/Jcla.20049

Mckinnon AJ, Tobolsky AV (1966) Structure and transition in solid state of a helical macromolecule. J Phys Chem 70:1453. doi:10.1021/J100877a018

Mezger T, Cantow HJ (1983a) Cellulose containing block copolymers.4. Cellulose triester macroinitiators. Angew Makromol Chem 116:13–27

Mezger T, Cantow HJ (1983b) Cellulose containing block copolymers. 5. Threeblock co-polymer syntheses via macroinitiator. Makromol Chem, Rapid Commun 4:313–320

Mezger T, Cantow HJ (1984) Cellulose-containing triblock copolymers—syntheses via cellulosic dithiodiaryl photoinitiators. Polym Photochem 5:49–56

Miyazawa T (1960) Perturbation treatment of the characteristic vibrations of polypeptide chains in various configurations. J Chem Phys 32:1647–1652. doi:10.1063/1.1730999

Nakagawa A, Kamitakahara H, Takano T (2012) Synthesis and thermoreversible gelation of diblock methylcellulose analogues via Huisgen 1,3-dipolar cycloaddition. Cellulose 19:1315–1326. doi:10.1007/S10570-012-9703-7

Papadopoulos P, Floudas G, Klok HA, Schnell I, Pakula T (2004) Self-assembly and dynamics of poly(γ-benzyl-L-glutamate) peptides. Biomacromolecules 5:81–91. doi:10.1021/bm034291q

Papadopoulos P, Floudas G, Schnell I, Aliferis T, Iatrou H, Hadjichristidis N (2005) Nanodomain-induced chain folding in poly(gamma-benzyl-L-glutamate)-b-polyglycine diblock copolymers. Biomacromolecules 6:2352–2361. doi:10.1021/Bm0501860

Pohjola L, Eklund V (1977) Polyurethane block copolymers from cellulose acetate. Pap Puu 3:117–120

Roche E, Chanzy H, Boudeulle M, Marchessault RH, Sundararajan P (1978) 3-dimensional crystalline-structure of cellulose triacetate-ii. Macromolecules 11:86–94. doi:10.1021/Ma60061a016

Sakaguchi M, Ohura T, Iwata T, Takahashi S, Akai S, Kan T, Murai H, Fujiwara M, Watanabe O, Narita M (2010) Diblock copolymer of bacterial cellulose and poly(methyl methacrylate) initiated by chain-end-type radicals produced by mechanical scission of glycosidic linkages of bacterial cellulose. Biomacromolecules 11:3059–3066. doi:10.1021/Bm100879v

Sanchez-Ferrer A, Mezzenga R (2010) Secondary structure-induced micro- and macrophase separation in rod-coil polypeptide diblock, triblock, and star-block copolymers. Macromolecules (Washington DC, U S) 43:1093–1100. doi:10.1021/ma901951s

Sanefuji T, Ando I, Inoue Y, Uematsu I, Shoji A (1985) Effect of pressure on the magnetic orientation of the poly(γ-benzyl L-glutamate) liquid crystal as studied by proton NMR under high pressure. Macromolecules 18:583–585. doi:10.1021/ma00145a048

Toriumi H, Uematsu I (1984) Optical properties of lyotropic poly(γ-benzyl L-glutamate) liquid crystals. Mol Cryst Liq Cryst 116:21–33. doi:10.1080/00268948408072493

Toriumi H, Kusumi Y, Uematsu I, Uematsu Y (1979) Thermally induced inversion of the cholesteric sense in lyotropic polypeptide liquid crystals. Polym J 11:863–869. doi:10.1295/polymj.11.863

Toriumi H, Minakuchi S, Uematsu Y, Uematsu I (1980) Helical twisting power of poly(γ-benzyl L-glutamate) liquid crystals in mixed solvents. Polym J (Tokyo) 12:431–437. doi:10.1295/polymj.12.431

Toriumi H, Minakuchi S, Uematsu I (1981) Concentration and temperature dependence of the helical twisting power of poly(γ-benzyl L-glutamate) liquid crystals in m-cresol. J Polym Sci Polym Phys Ed 19:1167–1169. doi:10.1002/pol.1981.180190715

Toriumi H, Yahagi K, Uematsu I, Uematsu Y (1983) Cholesteric structure of lyotropic poly(γ-benzyl L-glutamate) liquid crystals. Mol Cryst Liq Cryst 94:267–284. doi:10.1080/15421408308084262

Trent JS, Scheinbeim JI, Couchman PR (1983) Ruthenium tetraoxide staining of polymers for electron-microscopy. Macromolecules 16:589–598. doi:10.1021/Ma00238a021

Tsai ML, Chen SH, Marshall KL, Jacobs SD (1990) Thermotropic and optical properties of chiral nematic polymers. Int J Thermophys 11:213–223. doi:10.1007/bf00503872

Uematsu I, Uematsu Y (1984) Polypeptide liquid crystals. Adv Polym Sci 59:37–73

Vivatpanachart S, Tsujita Y, Takizawa A (1981) Gas permeability of the racemic form of poly(γ-benzyl glutamate). Makromol Chem 182:1197–1206

Wang K, Liang LY, Lin SL, He XH (2008) Synthesis of well-defined ABC triblock copolymers with polypeptide segments by ATRP and click reactions. Eur Polym J 44:3370–3376. doi:10.1016/J.Eurpolymj.07.042

Watanabe J, Uematsu I (1984) Anomalous properties of poly(γ-benzyl L-glutamate) film composed of unusual 7/2 helices. Polymer 25:1711–1717. doi:10.1016/0032-3861(84)90242-8

Weiss RA, Shao L, Lundberg RD (1992) Melt-processable polypeptide/ionomer molecular composites. Macromolecules 25:6370–6372. doi:10.1021/ma00049a039

Yagi S, Kasuya N, Fukuda K (2010) Synthesis and characterization of cellulose-b-polystyrene. Polym J (Tokyo, Jpn) 42:342–348. doi:10.1038/pj.2009.342

Zhou QH, Zheng JK, Shen ZH, Fan XH, Chen XF, Zhou QF (2010) Synthesis and hierarchical self-assembly of rod rod block copolymers via click chemistry between mesogen-jacketed liquid crystalline polymers and helical polypeptides. Macromolecules 43:5637–5646. doi:10.1021/Ma1007418